Classical Molecular Dynamics Study of [60]Fullerene Interactions with Silica and Polyester Surfaces

ARTICLE *in* THE JOURNAL OF PHYSICAL CHEMISTRY B · SEPTEMBER 2006

Impact Factor: 3.3 · DOI: 10.1021/jp0622886 · Source: PubMed

3 AUTHORS:

David J Henry
Murdoch University
53 PUBLICATIONS **1,244** CITATIONS
SEE PROFILE

E J Evans
BlueScope Steel
36 PUBLICATIONS **559** CITATIONS
SEE PROFILE

Irene Yarovsky
RMIT University
154 PUBLICATIONS **2,244** CITATIONS
SEE PROFILE

Classical Molecular Dynamics Study of [60]Fullerene Interactions with Silica and Polyester Surfaces

David J. Henry,[†] Evan Evans,[‡] and Irene Yarovsky*[,†]

School of Applied Sciences, RMIT University, GPO Box 2476V, Victoria, 3001, Australia, and BlueScope Steel Research, Port Kembla, Australia

Received: April 13, 2006; In Final Form: June 14, 2006

This study examines the interaction of neutral and charged fullerenes with model silica and polyester surfaces. Molecular dynamics simulations at 298 K indicate that van der Waals forces are sufficiently strong in most cases to cause physisorption of the neutral fullerene particle onto the surfaces. The fullerenes are unable to penetrate the rigid silica surface but are generally able to at least partially infiltrate the flexible polymer surface by opening surface cavities. The introduction of charge to the fullerene generally leads to an increase in both the separation distance and Work of Separation with silica. However, the charged fullerenes generally exhibit significantly closer and stronger interactions with polyester films, with a distinct tendency to absorb into the "bulk" of the polymer. The separation distance and Work of Separation of C_{60} with each of the surfaces also depend greatly on the sign, magnitude, and localization of the charge on the particle. Cross-linking of the polyester can improve resistance to the neutral fullerene. Functionalization of the polyester surface (F and OH substituents) has been shown to prevent the C_{60} from approaching as close to the polyester surface. Fluorination leads to improved resistance to positively charged fullerenes, compared to the unmodified polyester. However, hydroxylation generally enables greater adhesion of charged fullerenes to the surface due to H-bonding and electrostatic attraction.

1. Introduction

Polyesters represent an important class of polymers used as the basis of a number of industrial coatings. However, polyesters are generally hydrophobic and tend to attract hydrophobic contaminants, such as carbonaceous solids, which may deteriorate the performance and appearance of these coatings.[1] It is therefore of interest to investigate the interactions and mechanisms of carbonaceous contamination of polyester surfaces.

Biomass and fossil fuel burning are major sources of atmospheric carbonaceous particles. Depending on the nature of the fuel and the combustion conditions, the black carbonaceous residue can display a range of particle types with distinct properties including tar balls and soot. Tar balls have been identified by Pósfai et al.[2] as amorphous carbonaceous spherules with diameters typically between 30 and 500 nm. They note that tar balls, ∼90% carbon with traces of O, S, K, Cl, and Si, can be distinguished from soot by their morphology and lack of turbostratic microstructure. They also note that no reflections or even continuous rings are observed from electron diffraction. In comparison, several studies[3,4] have shown that the primary particles of soot are spherical with diameters of 20−30 nm and comprise an onion-shell structure composed of approximately 7−10 graphitic (001) planes, often surrounding an amorphous core. Ghzaoui et al.[5] note that diesel soot may be mixed with different mineral oxides inlayed in the main carbonaceous body and also often contains a significant proportion of noncombusted organic species deposited on the surface.We have previously used graphite[6,7] as a simple model of the surface of soot particles while our amorphous carbon[8] model provides a representation of tar ball type carbonaceous material. In our recent studies rigid and relaxed interfaces were constructed between these carbon models and model polyester and silica surfaces.[9] From these interfaces the Work of Separation (W_{sep}) and theoretical Work of Adhesion (W_{ad}) were calculated.

[60]Fullerenes with their spherical aromatic structure may also provide a convenient simple model of soot particles. There have been a number of studies investigating the deposition of fullerenes onto polymer surfaces.[10] However, these studies have generally been focused on immobilizing the C_{60} onto the surfaces, i.e., covalently bonding the fullerene to the polymer. For example, Birgulin et al.[10a] investigated [60]fullerene solid films deposited on polyacrylonitrile substrates by vacuum sublimation. They found that these polymer substrates were ideal for chemisorption of C_{60} via Diels−Alder cycloaddition of the fullerene to the unsaturated bonds of the polymer nitrile groups. Ren et al.[10b] prepared self-assembled C_{60} films by chemical adsorption onto an amino group-containing polyethyleneimine-coated silicon substrate.

There have been a number of studies investigating the separation and purification of fullerenes with chromatographic techniques.[11] Clearly the affinity of the fullerenes for the surface of the stationary phase relative to their solubility in the eluting solvent determines the effectiveness of the separation. Several reports have indicated that normal phase silica and alumina stationary phases can be used to separate fullerenes on a laboratory scale. In a related study, Piwonski et al.[12] studied C_{60} adsorption on mesoporous MCM-41 silica at room temperature using flow microcalorimetry and found that fullerene adsorption was completely reversible. These studies indicate that fullerenes have some affinity for silica surfaces. Alternatively,

* Address correspondence to this author. E-mail: irene.yarovsky@rmit.edu.au.
[†] RMIT University.
[‡] Bluescope Steel Research.

10.1021/jp0622886 CCC: $33.50
Published on Web 07/27/2006

TABLE 1: Average Partial Atomic Charges and Percentage Composition for the Principal Atom Types of Silica50, Polyester, Polyester75F, and Polyester75OH Surface Models

	Silica50		Polyester		Polyester75F		Polyester75OH	
atom type	charge	%	charge	%	charge	%	charge	%
O (silanol)	−0.728	2.8						
H (silanol)	+0.290	2.8						
O (siloxane)	−0.623	62.0						
Si	+1.229	32.4						
C (aromatic)			−0.060	11.7	−0.050	11.7	−0.053	11.4
C (alkyl)			−0.046	21.9	−0.037	2.0	−0.034	19.0
C−F, C−OH					+0.307	2.8	+0.180	2.2
C (carbonyl)			+0.597	3.7	+0.597	3.7	+0.597	3.6
O (carbonyl)			−0.450	3.7	−0.450	3.7	−0.450	3.6
O (ester)			−0.272	3.7	−0.272	3.7	−0.272	3.6
O (ether)			−0.320	1.3	−0.320	1.3	−0.320	1.3
O (hydroxyl)			−0.570	0.4	−0.570	0.4	−0.570	3.4
H (hydroxyl)			+0.410	0.4	+0.410	0.4	+0.410	3.4
H			+0.063	51.7	+0.064	48.0	+0.064	46.6
N			+0.432	1.5	+0.432	1.5	+0.432	1.5
F					−0.244	3.7		

there has been greater success in purifying fullerenes with aliphatic and aromatic reverse-phase stationary phases. Kartsova and Makarov[13] prepared fullerene-based stationary phases for gas chromatography. They found that the fullerene stationary phase is close in performance to nonpolar liquid phases, exhibiting high affinity for aromatic hydrocarbons and their functional derivatives as well as heterocyclic compounds, reflecting the electron-deficient polyene nature of C_{60}.

Effects of electrostatic charges on properties of carbon and mineral surfaces are important for many technological processes. For example, there is considerable interest in dry processing/separation of coal (carbonaceous material) from minerals. Electrostatic separation has been proposed[14] as a means of separating finely ground coal from mineral particles. Triboelectrification can be used to charge the particles which can then be separated by passing them through a high strength electric field. Ban et al.[14] investigated the effectiveness of this process for separation of carbon−silica mixtures. Another technological area for which the effect of electrostatic charge on particle adhesion is of particular interest is in electrophotography. In fact, there has been a lively debate in the literature[15] regarding the relative importance of van der Waals and electrostatic forces on toner adhesion with various substrates.

In the present study we use [60]fullerenes to model carbonaceous particles interacting with silica, polyester, and modified polyester surfaces using classical molecular dynamics. The strength of the interactions between the fullerenes and the selected surfaces is characterized by the Work of Separation and the average separation distance. The effects of fullerene charge on adsorption properties are also investigated.

2. Theoretical Procedures

A. Surface Models. The cross-linked polyester surface model (Polyester) was prepared by using the previously reported algorithm.[16] The structure is composed of polyester chains which contain on average 15 units of 2-butyl-2-ethyl-1,3-propanediol, 2 units of trimethylolpropane, and 16 units of isophthalic acid and these chains are cross-linked with tributoxymethylmelamine to give a cross-linked polymer structure with a density of 1.14 g cm^{-3}.

The base polyester surface was then modified to include additional functional groups on the $x-y$ surfaces with coverages of 4.7 residues per nm^2 (75 substituents per unit cell surface area, Polyester75), by replacement of the highest H atoms on the polymer surface. The functional groups introduced were hydroxyl (Polyester75OH) and fluorine (Polyester75F). As a result, the total number of atoms for the F modified system is equivalent to that of the base polyester, while for the Polyester75OH system the total number increases by 75 atoms.

The silica model used in the present study is a realistic model of a vitreous silica surface based on the work of Garofalini and co-workers[17] and has been modified as reported previously[18] to produce a hydroxylated surface. In the current study, the silica model was prepared with surface hydroxylation of 3.1 OH groups per nm^2 (50 hydroxyl groups per unit cell area, Silica50), which represents a partially hydrated silica surface. Zhuravlev[19] reports that a completely hydrated silica surface has a silanol density of ∼5.0 OH groups per nm^2. For all subsequent simulations the surface silanol groups remained free to move while the underlying silica was held in a fixed geometry.

For C_{60}, each of the carbon atoms is assigned a partial atomic charge of 0.000 e to maintain overall neutrality. For C_{60}^+ and C_{60}^-, each carbon is assigned a partial charge of ±0.017 e, respectively, while for C_{60}^{3+} and C_{60}^{3-}, each carbon was assigned a partial charge of ±0.050 e, respectively. An additional charged fullerene ($C_{60}^{3-(local)}$) particle was prepared in which three −1.0 e charges were assigned to alternate carbons of a single six-membered ring, thereby localizing the charge to a single "face" of the fullerene. While this might seem like an unrealistic arrangement, it provides a simple model of a carbonaceous particle with a localized "charge defect" without actually destroying the structural integrity of the model particle. Interestingly, Gady et al.[15a] investigated contact electrification and the interaction force between a micrometer size polystyrene sphere and a graphite surface. Using two independent techniques (static and dynamic modes of AFM) they discovered that the interaction force is dominated at long range by an electrostatic force arising from localized charges triboelectrically produced on the sphere when it makes contact with the substrate. The average charges for the principal atom types of each model are presented in Table 1.

All surface models were created to be approximately the same size with an area of 40 × 40 $Å^2$ (x and y directions) and a thickness of approximately 18 Å (z direction). Each system was formed by placing the fullerene particles at a fixed initial distance from the surface boundary, which is defined as described in Section 2B and illustrated in Figure 1. The simulation box was further extended to 150.0 Å in the z-direction

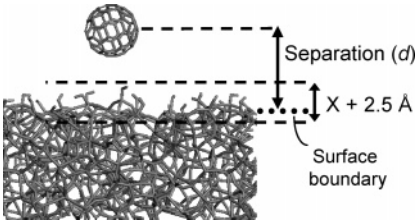

Figure 1. Schematic diagram of the fullerene−polyester interface and the representation of the definition of the surface boundary and separation distance.

to create a vacuum separation to prevent interactions occurring across adjacent cells, due to the 3D periodic boundary conditions imposed on the system. As a result, quasi-2D periodic systems were created.

B. Computational Details. The potential energy for each system was calculated with use of the COMPASS force field.[20] During molecular dynamics nonbonded interactions were calculated with an atom-based procedure, using a 15.50 Å cutoff, a spline width of 5.00 Å, a buffer of 2.00 Å, and a long-range tail correction. Simulations were performed in the NVT ensemble, equilibrated for 500 ps with data acquisition for 500 ps, using 1.0 fs time steps. The temperature was maintained at 298 K with the Andersen thermostat[21] with a collision ratio of 1.0. The separation distance was calculated as the distance from the center of mass of the fullerene to the surface boundary, as defined below. For each system, a minimum of five separate molecular dynamics simulations were run with the fullerene particle starting in different locations (x, y coordinates) relative to the silica and polyester surfaces. At the completion of each of these molecular dynamics simulations, energy minimization was performed on the system with the Cell Multipole procedure with an update width of 5.00 Å and a convergence limit of 0.04 kJ mol^{-1} $Å^{-1}$. These energy values were used for adhesion energy calculations.

In each case the molecular dynamics simulations were started with the center of mass of the C_{60} located 8.0−10.0 Å from the silica or polyester surface to ensure that the interactions between the particle and the surface are within the chosen cutoff distance.

Although all surfaces were created to be approximately equal in thickness (18 Å), the boundary of the surfaces was difficult to identify due to the atomic roughness in the surface profiles. The amorphous nature of the silica and polyester surfaces presented an ambiguity in assigning the exact surface boundary; therefore, for the unmodified polyester model it was arbitrarily calculated as the $x-y$ plane having a z value equal to the average z for all atoms in the leading 2.5 Å of the surface. For the functionalized polyester and silica models, where the surface substituents increase surface roughness, the boundary was determined to be represented by the $x-y$ plane having z equal to the average z for all atoms comprising the surface modifications plus the atoms in the leading 2.5 Å of the bulk (Figure 1).

The Work of Separation (W_{SEP}) for the interaction of a single fullerene with a silica or polyester surface was calculated on the minimized final structure according to

$$W_{SEP} = (E_{SURF} + E_{FUL} - E_{SYS})/A_{FUL} \quad (1)$$

where E_{SURF} is the energy of the surface, E_{FUL} is the energy of the fullerene, E_{SYS} is the total energy of the minimized system, and A_{FUL} is the surface area of the fullerene.

3. Results and Discussion

In a typical simulation the fullerene is attracted to the surface and then proceeds to "roll" across the surface until an equilibrium interaction/position is established. Table 2 contains average separation distances (d) and Work of Separation (W_{SEP}) values for both neutral and charged C_{60} particles interacting with silica and polyester surfaces. The Work of Separation values are the average of W_{SEP} for a minimum of five individual runs. The specific details of the interactions with the selected surfaces will be discussed in more detail below.

A. C_{60} on Silica. Our partially hydrated silica surface has a distribution of silanol and siloxane groups across the surface leading to hydrophilic and hydrophobic regions, respectively, in agreement with experiment.[22] [60]Fullerene adhesion is generally maximized in regions of lower hydroxyl density, enabling closer interactions between the atoms of the fullerene and the underlying silica. For several of the simulations, the fullerene initially located directly above the surface OH groups migrates to "bare" regions of the surface adjacent to OH groups, enabling VDW interactions not only with the underlying silica (z-direction) but also with the local OH groups ($x-y$ direction).

The average separation distance for the Silica50/C_{60} system is significantly larger than the corresponding d for C_{60} with the polyester surfaces (Table 2). In addition to this, the W_{SEP} is lower than for the Polyester/C_{60} systems, in agreement with our adhesion studies[6,7] and in qualitative agreement with experiment.[23]

With the introduction of a single delocalized positive charge to the fullerene, there is a significant increase in the W_{SEP}. This indicates that a significant electrostatic interaction now exists leading to greater attraction between the fullerene and the silica surface. In fact electrostatic forces now contribute 46% to the total adhesion energy. Inspection of the individual simulations indicates that the charged fullerenes now migrate to regions with higher local hydroxyl concentration and generally "hover" adjacent to, or over the hydroxyl oxygen atoms, contributing to the increase in d.

Interestingly, the $g(r)$ for carbon in C_{60}^{+} to silanol oxygen (Figure 2) exhibits almost no change in magnitude but a very slight shift to shorter separation. This suggests that the electrostatic attraction between the negatively charged oxygen atoms and the positive carbon atoms is sufficient to significantly increase W_{SEP} and to partially overcome the short-range VDW repulsion. Not surprisingly, the $g(r)$ for carbon to hydrogen exhibits a significant shift to larger separations, reflecting the electrostatic repulsion between these positively charged atoms and the ability of the hydrogens to orient away from the fullerene

TABLE 2: Average Separation Distance (d, Å) and Work of Separation (W_{SEP}, mJ m^{-2}) for Neutral and Charged C_{60} with Silica and Polyester Surfaces

	C_{60}		C_{60}^{+}		C_{60}^{3+}		C_{60}^{-}		C_{60}^{3-}		$C_{60}^{3-(local)}$	
	d	W_{SEP}	d	W_{SEP}	d	W_{SEP}	d	W_{SEP}	d	W_{SEP}	d	W_{SEP}
Silica50	4.7	49.4	5.0	90.7	5.2	188.7	4.6	32.5	5.2	68.7	5.8	121.8
Polyester	2.8	79.4	1.8	121.3	−0.8	455.7	1.1	104.0	−0.3	275.8	0.6	341.1
Polyester75F	3.1	83.0	2.7	111.2	1.3	383.6	2.6	94.1	−1.4	391.8	−0.4	513.9
Polyester75OH	3.4	78.5	2.7	106.9	1.2	467.6	2.2	120.8	0.2	456.0	1.5	909.2

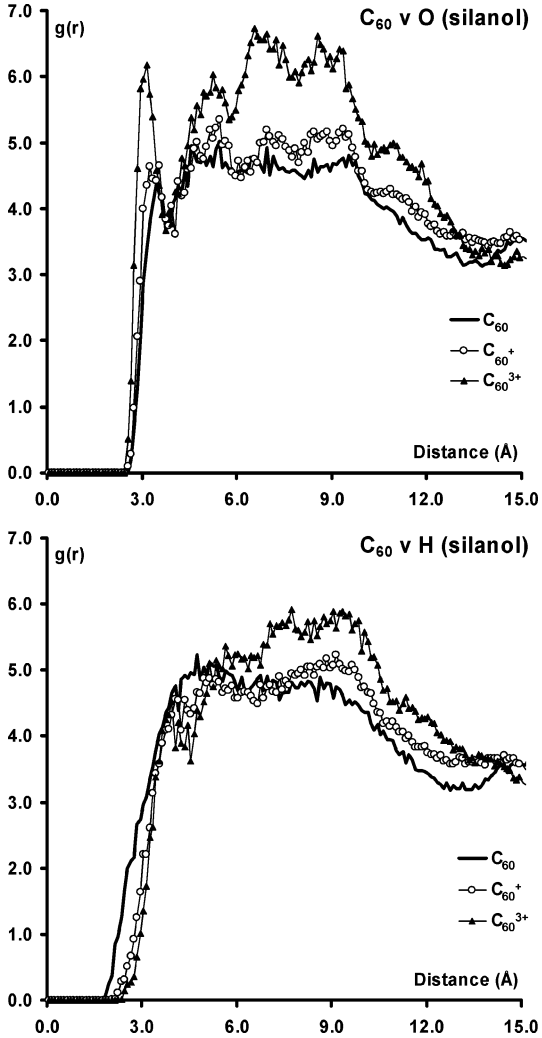

Figure 2. Radial distribution functions for C_{60}, C_{60}^{+}, and C_{60}^{3+}/Silica50 systems.

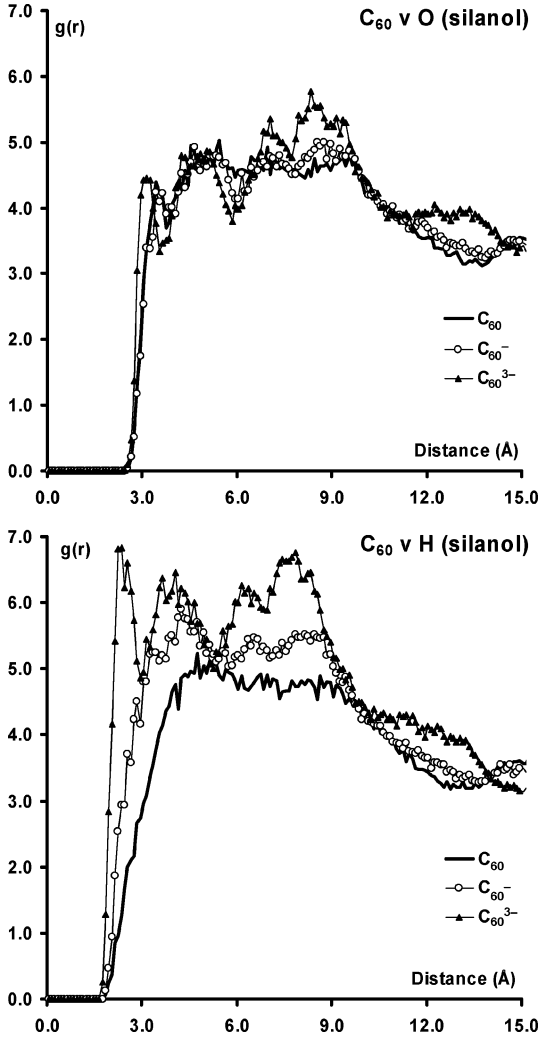

Figure 3. Radial distribution functions for C_{60}, C_{60}^{-}, and C_{60}^{3-}/Silica50 systems.

due to their greater mobility. Electrostatic repulsion between the fullerene and the positive silicon atoms may contribute to the slight increase in d but this is not evident in the $g(r)$ for these atom types.

The effects observed for C_{60}^{+} are further accentuated in the C_{60}^{3+}/Silica50 system where W_{SEP} is ~3.8 times greater than for neutral C_{60} and d is 0.5 Å longer. Electrostatic forces now make the major (80%) contribution to adhesion. The $g(r)$ for carbon to silanol oxygen (Figure 2) now demonstrates a significant increase in the first peak with a further shift to shorter separation. Likewise, the $g(r)$ for carbon to hydrogen exhibits a further slight shift to larger distance.

In contrast, the introduction of a single (delocalized) negative charge to the fullerene leads to a 34% reduction in W_{SEP} with Silica50. The adhesion is generally stronger in regions of lower silanol density with relatively little change in d. This suggests that van der Waals forces remain dominant, holding the particle close to the surface while the repulsive electrostatic interaction is largely directed "parallel" (i.e., in the $x-y$ plane) to the surface, between the partial negative charges of the fullerene atoms and the oxygen atoms of the surface silanols. Surprisingly, there is no noticeable difference in the fullerene radial distribution function with the oxygen atoms of the surface OHs (Figure 3). In contrast, we do see the expected increase in $g(r)$ at shorter distances for C_{60}^{-} carbon atoms with hydrogen. This is not surprising, since the hydroxyl hydrogens, with positive partial atomic charges are able to freely rotate about the oxygen atoms and are attracted toward the partial negative charges of the C_{60}^{-} atoms. As a consequence, there is a subtle balance of the attractive VDW forces between C_{60}^{-} and the hydroxyl oxygen and hydrogen atoms, the attractive electrostatic forces between C_{60}^{-} and the hydrogen atoms, and the repulsive electrostatic forces between C_{60}^{-} and the hydroxyl oxygen atoms. The W_{SEP} and the RDFs suggest that the attractive forces are dominant. Nevertheless, the repulsive electrostatic force is sufficient to significantly reduce the interaction energy.

There is essentially no difference in the $g(r)$ for C_{60} and C_{60}^{-} carbon atoms with bulk silica oxygen or silicon atoms, consistent with the similarity of the d values for each of these systems.

Interestingly, for the C_{60}^{3-}/Silica50 system there is now an increase in d (0.6 Å) and a 40% increase in W_{SEP}, relative to C_{60}/Silica50. However, van der Waals forces still remain the dominant (72%) contributor to intermolecular adhesion. The $g(r)$ for carbon to hydrogen exhibits a significant shift to shorter distance with a peak at 2.25 Å, while the $g(r)$ for carbon to hydroxyl oxygen exhibits a peak at 3.15 Å, indicative of a weak hydrogen bond type interaction (Figure 3). The hydroxyl hydrogens are generally located "high" on the silica surface; therefore, the increased hydrogen bonding actually lifts the fullerene from the surface leading to the increased d.

This type of interaction is further emphasized in the $C_{60}^{3-(local)}$/Silica50 system where the W_{SEP} value indicates a strong

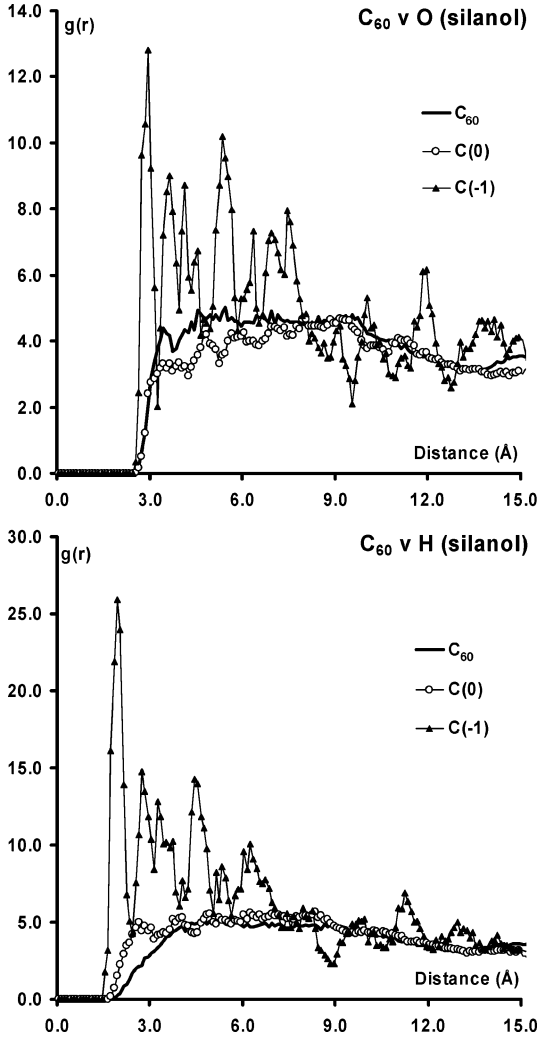

Figure 4. Radial distribution functions for the neutral (C(0)) and charged (C(1)) atoms of $C_{60}^{3-(local)}$/Silica50 systems compared with C_{60}/Silica50.

interaction between the particle and the surface with an increased *d*. In comparison with the delocalized C_{60}^{3-} system, electrostatic forces represent 70% of the intermolecular force while van der Waals forces contribute only 30%. Inspection of the individual simulations demonstrates that once the $C_{60}^{3-(local)}$ fullerene has come in contact with the surface, the charged region becomes anchored to the nearby OH groups by H-bonding-type interactions. This is demonstrated in the RDFs (Figure 4), with significant peaks at 1.95 and 2.95 Å for the charged carbons to silanol hydrogen and oxygen, respectively.

Our results indicate that there is an inherent small attraction between C_{60} and a partially hydrated silica surface due to van der Waals forces. In fact this weak affinity for silica has enabled experimentalists to use silica gel stationary phases for the separation and purification of fullerenes on the laboratory scale.[11a,c,d] However, as Wu et al.[11d] note, the effectiveness of the separation is dependent on the activity of the silica. Piwonski et al.[12] used flow microcalorimetry to study the adsorption of C_{60} from toluene solutions on mesoporous MCM-41-type silica at room temperature. They reported a molar enthalpy of adsorption of -3000 kJ mol^{-1} that is considerably higher than our theoretical estimates of $\sim$100 kJ mol^{-1} and is in fact approximately 10 times higher than that for chemisorption on active carbon. However, adsorption−desorption studies rule out the possibility of chemisorption and indicate that the fullerenes are retained on the silica by weak solid−solute interactions. They conclude therefore that the large enthalpy is the result of hydrodynamic effects due to the flow of solution through the narrow cylindrical channels.

Our calculations also show that the introduction of charge to the fullerene generally leads to increased adhesion with silica. Ban et al.[14] were able to separate a physical mixture of silica and carbon with >90% efficiency by tribocharging the particles (silica negative and carbon positive) and passing it through an electric field. However, they noted that the effectiveness of the separation is impeded by the accumulation of positive or no charge on the silica. Our calculations indicate that neutral silica (which would not be deflected in an electric filed) has a net negative surface charge and therefore has increased attraction to positively charged carbon particles, which would impede separation of these particles.

B. C_{60} on Polyester. The average separation distance for the Polyester/C_{60} system indicates that the fullerene particle comes into much closer contact with the polyester surface than the silica surface, in conjunction with a significant increase in the Work of Separation. This is in full agreement with the observation that fullerenes have a greater affinity for alkyl and aromatic stationary phases compared with silica.[11c,e,g]

Close inspection of individual simulation runs indicates some variability in the fullerene/polyester interactions with starting location with respect to the polyester in the *x*,*y* direction. While the polyester has an overall cross-linking density of 8.8×10^{-4} groups per Å^3, within the model surface there are regions with significant cross-linking, which are therefore more rigid, and regions with little or no cross-linking, which exhibit significant mobility at 298 K. Noticeably, if the C_{60} adsorbs in regions where the cross-linking density is high, the average separation distances are larger (i.e., there is less intrusion of the fullerene into the surface), while the reverse is true in regions with little or no cross-linking. This indicates that one method of improving the resistance of polyester surfaces to carbon particle contamination is to increase the surface rigidity by, for example, increasing the cross-linking density.

Radial distribution functions between the carbon atoms of C_{60} and the component atoms of the polyester do not exhibit correlations, indicating that the interactions are nonspecific (Figure 5).

The W_{SEP} for C_{60}^+ with Polyester is 1.5 times greater than that for the neutral fullerene and there is a significant decrease in *d* (1.0 Å), indicating that the positively charged particles have an increased affinity for the polyester surfaces. The RDFs (Figure 5) with the negatively charged aromatic carbon, carbonyl oxygen, and nitrogen atom types exhibit slight shifts to shorter separations combined with increased intensity at longer separations, reflecting the electrostatic attraction. There is relatively little change in the RDF for alkyl carbon, despite the partial negative charge and large percentage composition (Table 1). The increased intensity at intermediate and long separations in positively charged carbonyl carbon and hydrogen most likely reflects the increased attraction to the adjoining carbonyl oxygen and aromatic carbon atoms, respectively.

The interaction of C_{60}^{3+} with the polyester surface leads to an extremely large increase in W_{SEP} and a further significant decrease in *d* (1.0 Å). It is clear from the negative value of *d* that the C_{60}^{3+} particles become embedded in the polyester films at 298 K. Inspection of the individual simulation runs indicates that even in the more rigid cross-linked regions, there is significant penetration of the surface by the triply charged fullerene, possibly reflecting the increased electrostatic attraction to the negatively charged nitrogen atoms. The RDF plots also

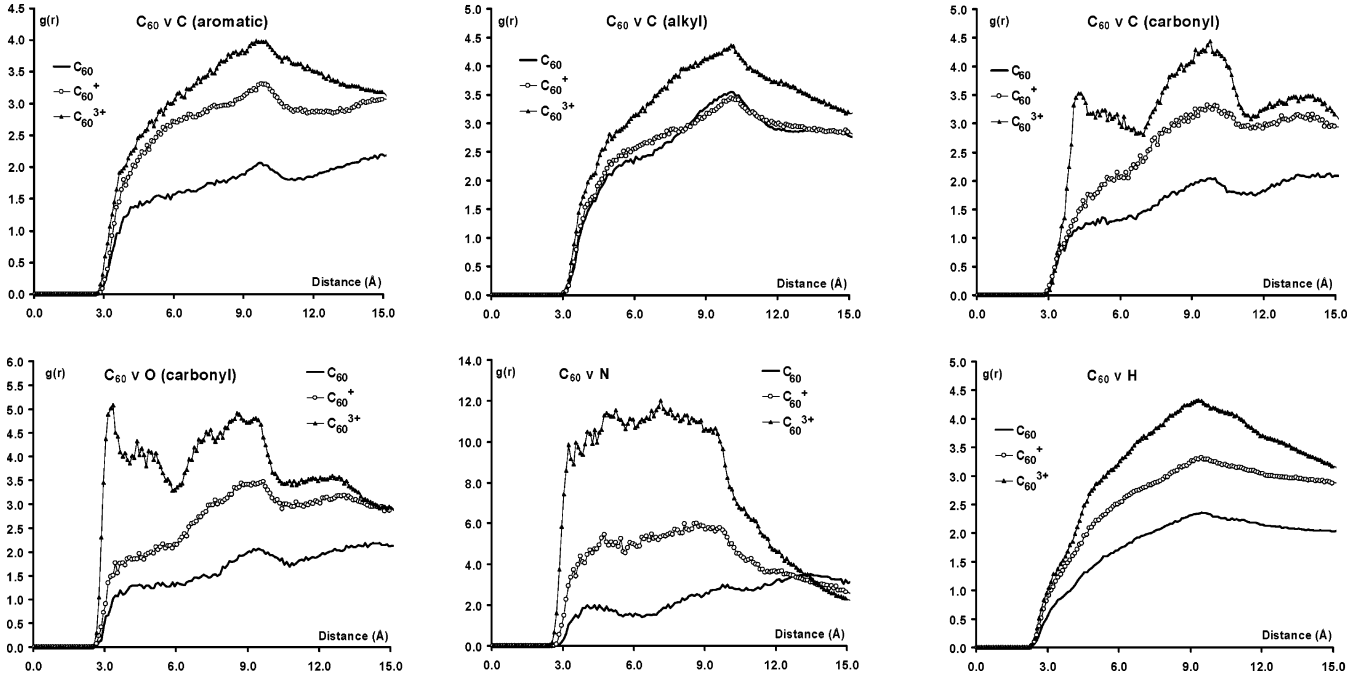

Figure 5. Radial distribution functions for C_{60}, C_{60}^{+}, and C_{60}^{3+}/Polyester systems.

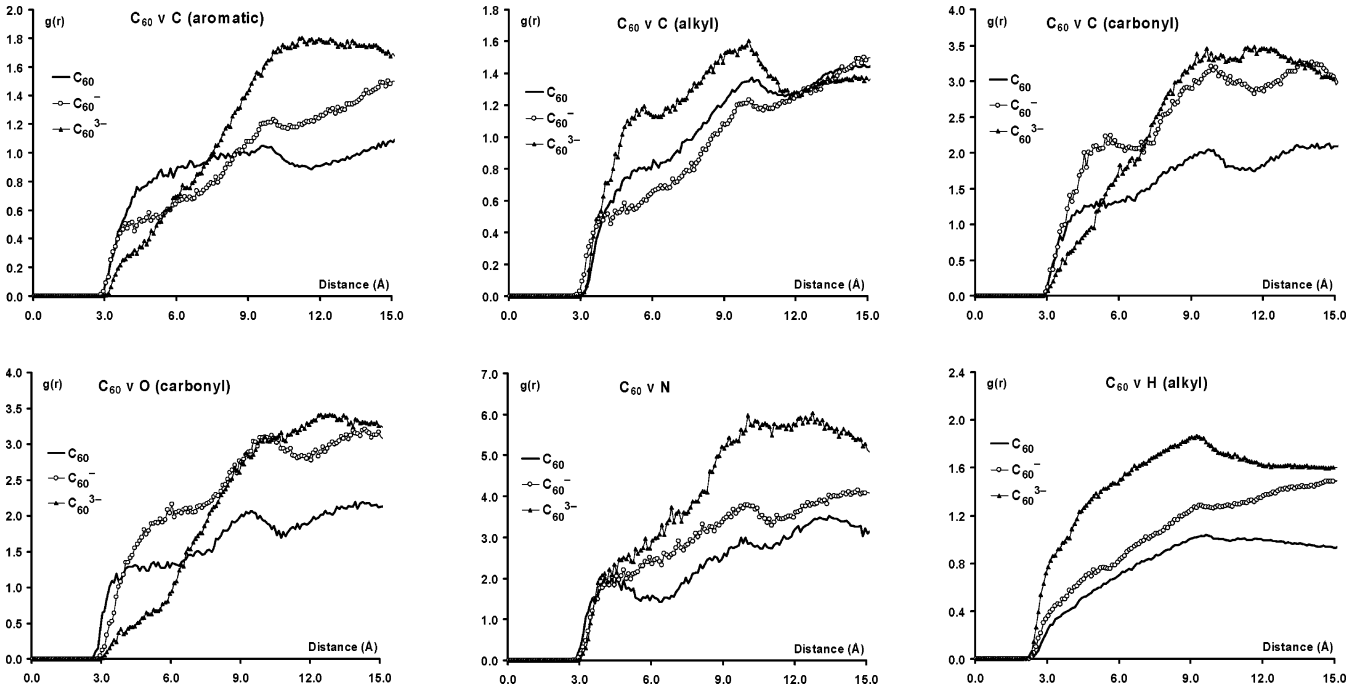

Figure 6. Radial distribution functions for C_{60}, C_{60}^{-}, and C_{60}^{3-}/Polyester systems.

demonstrate that there is increased attraction to the negatively charged aromatic carbon and carbonyl oxygen atom types particularly at intermediate to long range (>4.0 Å).

Interestingly, when a single negative charge is introduced to the fullerene, there is also an increase in the magnitude of W_{SEP} (31%) and a larger decrease in d (1.7 Å) than observed for C_{60}^{+}. The RDFs (Figure 6) indicate that one of the most significant interactions occurs for carbonyl oxygen with a shift to longer separation, reflecting the significant electrostatic repulsion between these atom types. There is little difference in the RDFs with the negatively charged aromatic and alkyl carbon at short distances (<4.0 Å), indicating that van der Waals forces dominate these particular interatomic interactions. There is a gradual increase in attraction between C_{60}^{-} and hydrogen with increased distance. The RDF with nitrogen exhibits an extremely small shift to longer separation due to electrostatic repulsion.

For the C_{60}^{3-}/Polyester system there is a further increase in W_{SEP} and a decrease in separation d (1.4 Å). The negatively charged carbonyl oxygen atoms clearly repel the charged fullerene, while the electrostatic interaction has increased sufficiently for the $g(r)$ for aromatic carbon to also exhibit a shift to longer distances (Figure 6). The RDF for positively charged hydrogen indicates increased attraction but the $g(r)$ for the negatively charged alkyl carbon again shows little change at shorter distances.

Localizing the three negative charges on one six-membered ring of the fullerene leads to an interesting result. The calculated W_{SEP} is larger than that for the delocalized C_{60}^{3-} but there is

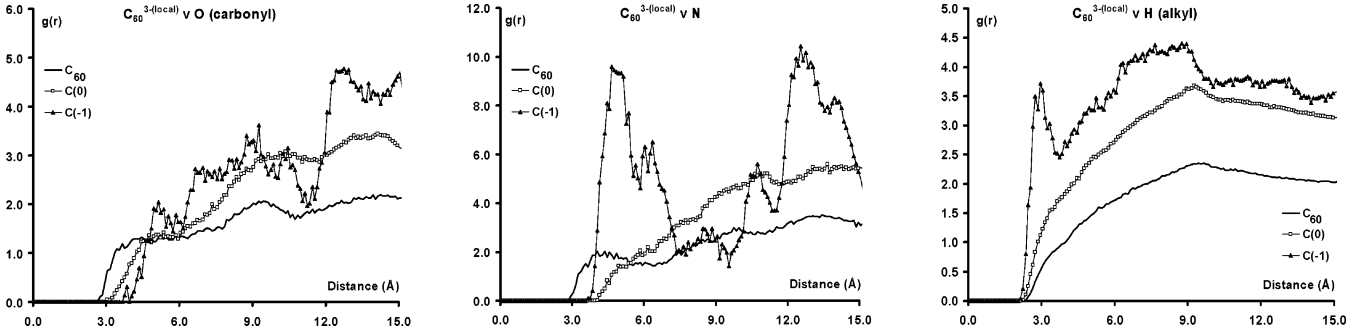

Figure 7. Radial distribution functions for the neutral (C(0)) and charged (C(−1)) atoms of $C_{60}^{3-(local)}$/polyester systems compared with C_{60}/Polyester.

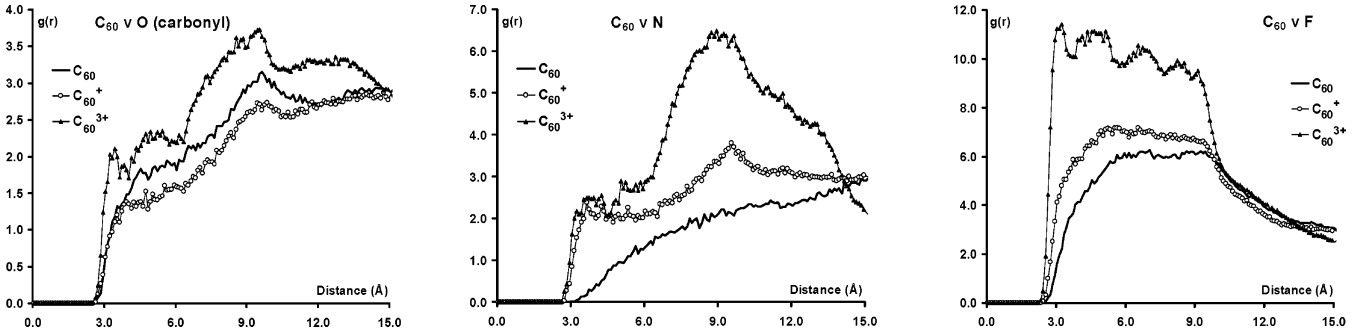

Figure 8. Radial distribution functions for C_{60}, C_{60}^{+}, and C_{60}^{3+}/Polyester75f systems.

an increase in *d*. Zhou et al.[15e] note that a point charge near the contact area can dominate the total adhesion force at small distances. Clearly, the charge distribution on the adhering particle has a strong influence on adhesion. This observation is supported by our theoretical calculations. The RDFs (Figure 7) indicate significant repulsion between the negatively charged carbon atoms (C(−1)) of the fullerene and the negatively charged carbonyl oxygen atoms. The nitrogen RDF also exhibits displacement to larger separation. Interestingly, the $g(r)$ for the negatively charged atoms displays two intense regions separated by approximately the diameter of the fullerene, suggesting that the charged region adopts specific orientations within the polymer surface. The hydrogen RDF exhibits a peak at ∼3.0 Å due to electrostatic attraction to the negatively charged carbon of $C_{60}^{3-(local)}$.

As noted in the Introduction, there has been considerable debate as to the relative importance of electrostatic and surface (VDW) forces on the adhesion of toner particles to photoconductors.[15] While our systems were not designed to model toner/photoconductor adhesion they provide some general insights into carbonaceous particle adhesion to polyester surfaces. It is clear that van der Waals forces provide significant adhesion between neutral fullerene particles and a neutral polyester surface. The introduction of a single delocalized positive or negative charge to the fullerene leads to significant increases in adhesion with the neutral polyester surface. However, the van der Waals forces remain the dominant intermolecular force contributing 78% and 82% of the total adhesion force for C_{60}^{+} and C_{60}^{-}, respectively. For C_{60}^{3+} and C_{60}^{3-} the situation is reversed with electrostatic forces contributing 71% and 65%, respectively, to the total intermolecular adhesion. Localization of a negative charge to a small region of the fullerene appears to lead to stronger attraction than for the equivalent delocalized charge and an increased electrostatic contribution of ∼77%.

Micrometer-size polyester toner particles used in electrophotography are often coated with nanometer-size silica particles to adjust adhesion and enhance flow. Rimai et al.[15f] suggested that asperities generated by the silica affect toner particle adhesion by altering nonelectrostatic interactions (e.g., van der Waals interactions). Our W_{SEP} results indicate that there is in fact a weaker van der Waals attraction between a neutral fullerene and silica compared with polyester. In addition to this, the W_{SEP} values for the charged fullerene/silica systems are all lower than the corresponding charged fullerene/polyester systems.

C. C_{60} on Fluorinated Polyester Surfaces. Functionalization of the polyester surface with fluorine groups leads to an increase in the average separation distance and a marginal increase in the Work of Separation relative to the unmodified polyester (Table 2). Close inspection of individual simulation runs indicates that the increased resistance of the cross-linked regions is slightly enhanced by the presence of fluorine surface functional groups. This finding is in agreement with our adhesion studies[7,9] which indicate that low levels of functionaliztion on rigid polyester surfaces, leading to increased atomic roughness, can reduce adhesion to graphite and amorphous carbon.

For the C_{60}^{+}/Polyester75F system, we observed a 34% increase in W_{SEP} and a slight decrease in *d* relative to C_{60}/Polyester75F. The increase in magnitude of W_{SEP} is slightly smaller than that observed in the corresponding unmodified polyester systems, as is the decrease in *d*. The electrostatic contribution to the adhesion energy decreases only slightly from 35% in the unmodified system to 33% in the fluorinated system. In contrast, for the C_{60}^{3+}/Polyester75F system, W_{SEP} is ∼4.6 times greater than for the neutral system and the electrostatic contribution increases to 77% of the total intermolecular force. The separation for the C_{60}^{3+}/Polyester75F system is also significantly shorter.

While the $g(r)$ for carbonyl oxygen to C_{60}^{+} shows no change at shorter separations (Figure 8) from neutral C_{60}, the $g(r)$ for C_{60}^{3+} exhibits the expected shift to shorter separation. Interestingly, the magnitude of the peak at ∼3.0 Å is significantly smaller than the corresponding peak in the Polyester/C_{60}^{3+} system. The RDFs for C_{60}^{+} and C_{60}^{3+} indicate that there is also

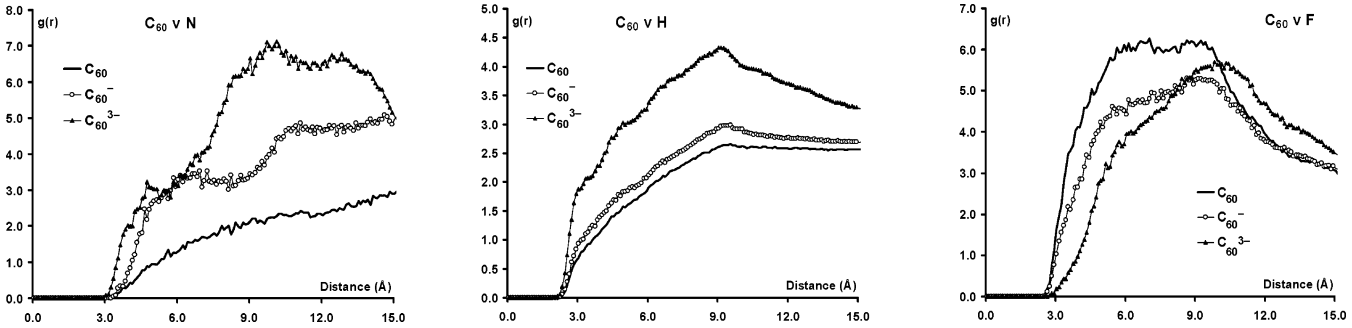

Figure 9. Radial distribution functions for C_{60}, C_{60}^-, and C_{60}^{3-}/Polyester75F systems.

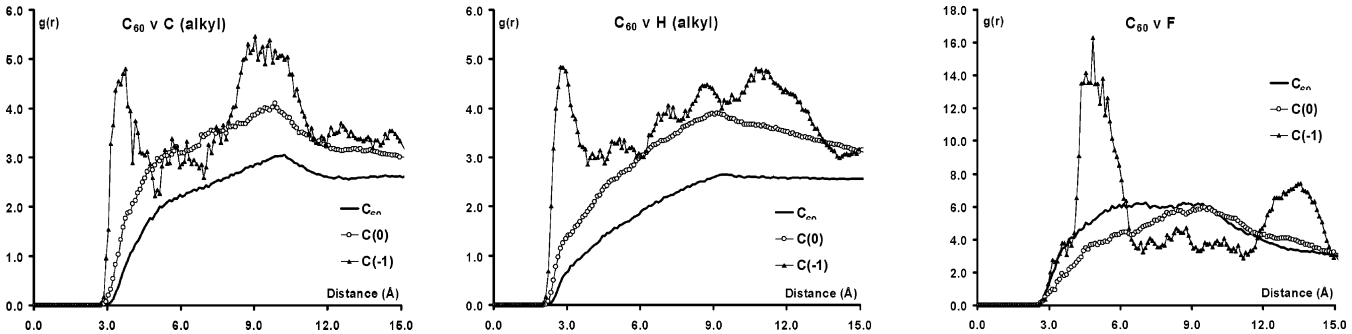

Figure 10. Radial distribution functions for the neutral (C(0)) and charged (C(1)) atoms of $C_{60}^{3-(local)}$/Polyester75F systems compared with C_{60}/Polyester75F.

increased attraction to negatively charged nitrogen and fluorine compared with C_{60}.

When a single negative charge is introduced to the fullerene, there is only a 13% increase in W_{SEP} but a noticeable decrease in d (0.5 Å). Interestingly, for the C_{60}^{3-}/Polyester75F system, the W_{SEP} value is similar in magnitude to that observed for C_{60}^{3+}/Polyester75F but the d value indicates that the fullerene penetrates the polymer surface to a much greater extent. Our results indicate that the Polyester75F surface exhibits a slightly increased resistance to C_{60}^- compared to the unmodified polyester. However, C_{60}^{3-} experiences increased adhesion to Polyester75F compared to Polyester.

The RDFs for the negatively charged fullerenes (Figure 9) exhibit the expected increases in $g(r)$ at short distance for the positively charged hydrogen atoms. The magnitude of the $g(r)$ curves for hydrogen is greater for Polyseter75F than for Polyester. The RDF for fluorine exhibits the expected displacement to larger separation due to electrostatic repulsion.

The calculated W_{SEP} for the $C_{60}^{3-(local)}$/Polyester75F system is considerably higher than that for the corresponding delocalized system. This interaction is largely dominated by electrostatic forces (85%). However, the separation distance indicates that there is significantly less penetration of the fullerene into the polyester surface.

The RDFs also show that there is increased attraction between the negatively charged carbon atoms of the fullerene (C(−1)) with the positively charged alkyl carbon and hydrogen atoms. Interestingly, the neutral carbon atoms of $C_{60}^{3-(local)}$ also exhibit increased interaction to the alkyl carbon and hydrogen atoms of the polymer compared with neutral C_{60}. However, this may only reflect the significantly shorter d value. The large peak in the fluorine RDF does not indicate an increased attraction between these negatively charged atoms but rather reflects the increased attraction to the adjacent positively charged carbon and hydrogen atoms.

D. C_{60} on Hydroxylated Polyester Surfaces. Functionalization of the polyester surface with hydroxyl groups leads to essentially no difference in W_{SEP} of C_{60} relative to the base polyester. However, there is an increase (0.6 Å) in separation distance d. This suggests that the fluorine and hydroxyl substituents "hold" the fullerene particle at slightly greater separations from the surface. The average d and W_{SEP} values reflect the balance between stronger short range (close contact) repulsive forces and stronger intermediate range attractive forces of fluorine and oxygen, compared with hydrogen. Once again we note that the resistance to the neutral fullerene is greatest in regions combining both surface functionalization and cross-linking.

The interaction of C_{60}^+ with the Polyester75OH surface is stronger than that for the neutral fullerene, with a 36% increase in W_{SEP} and a 0.7 Å decrease in d. The W_{SEP} for C_{60}^+/Polyester75OH is also slightly smaller than that for the corresponding interactions of C_{60}^+ with Polyester and Polyester75F indicating slightly increased resistance. However, for the C_{60}^{3+}/Polyester75OH system there is a significant increase in W_{SEP} and decrease in d (0.4 Å), indicating increased adhesion of C_{60}^{3+} relative to both the unmodified and fluorinated polyesters. The RDFs indicate that this is due to increased attraction to the negatively charged hydroxyl oxygen atoms at the surface of the polymer. As for Polyester75F, the magnitude of the carbonyl oxygen peak for C_{60}^{3+} is significantly smaller than that for Polyester.

The C_{60}^-/Polyester75OH system also exhibits a significant increase in W_{SEP} and decrease in d relative to the neutral C_{60}/Polyester75OH system. Noticeably, C_{60}^- exhibits a stronger adhesion to Polyester75OH than to the unmodified and fluorinated polyesters. For C_{60}^{3-}/Polyester75OH there is a further significant increase in W_{SEP} and decrease in d indicating increased adhesion by the fullerene. The RDFs (Figure 12) indicate that this is due to strong H-bonding interactions with the surface hydroxyl.

The $C_{60}^{3-(local)}$/Polyester75OH system exhibits the largest W_{SEP} value of all of the systems considered. The RDFs (Figure 13) indicate that there is a strong specific interaction between

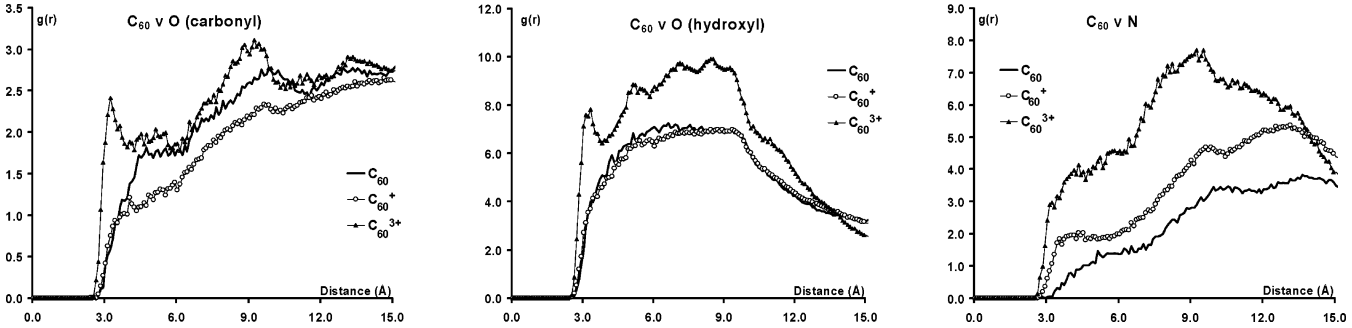

Figure 11. Radial distribution functions for C_{60}, C_{60}^{+}, and C_{60}^{3+}/Polyester75OH systems.

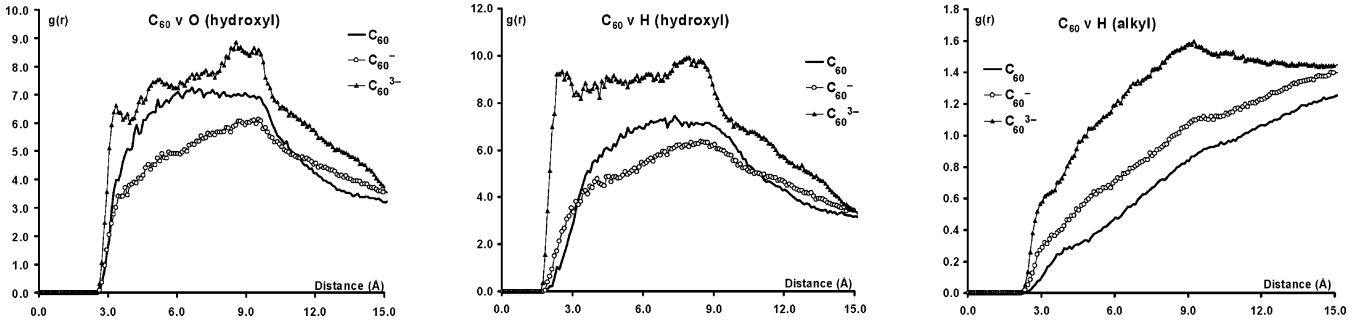

Figure 12. Radial distribution functions for C_{60}, C_{60}^{-}, and C_{60}^{3-}/Polyester75OH systems.

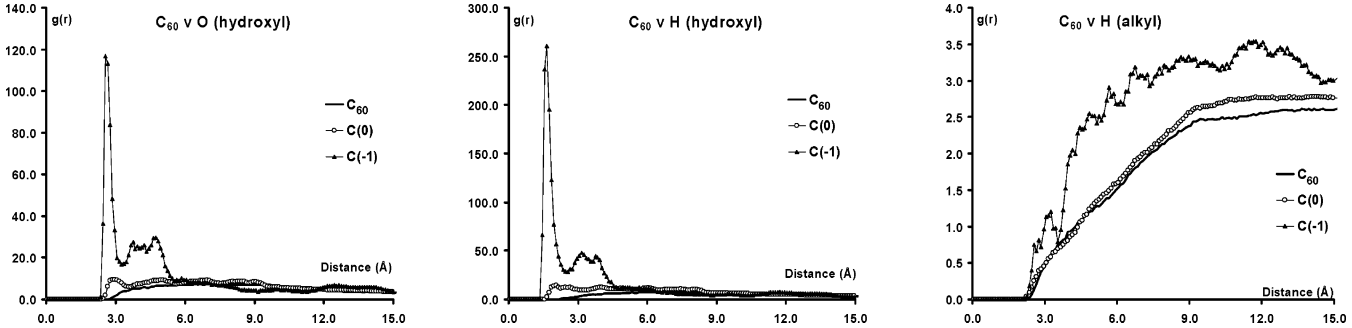

Figure 13. Radial distribution functions for the neutral (C(0)) and charged (C(1)) atoms of $C_{60}^{3-(local)}$/Polyester75OH systems compared with C_{60}/Polyester75OH.

the charged atoms of the fullerene and the hydroxyl groups of the polyester surface. There are also strong electrostatic interactions with the positively charged aromatic carbon and hydrogen atoms of the surface.

4. Conclusions

This study examined the interaction of neutral and charged fullerenes with model silica, polyester, and modified polyester surfaces using classical molecular dynamics simulations at 298 K. van der Waals forces are generally sufficiently strong to draw a neutral fullerene particle down onto both the silica and polyester surfaces. However, the interaction of C_{60} with both standard and modified polyesters is significantly greater than that with the silica surface.

Adhesion of the neutral C_{60} to silica is generally maximized in the "bare" hydrophobic regions of the surface. For the base polyester, adhesion is maximized in regions with little or no cross-linking in close proximity to the polyester surface adsorption site. Functionalization of the polyester surface (F and OH substituents) leads to a significant increase in separation distance so that while the attractive interactions are similar, the substituents "hold" the fullerene at slightly greater distance from the surface.

For all of the systems, the average separation distance (d) and Work of Separation (W_{SEP}) of the fullerene depends greatly on the charge on the particle. The interaction of a singly charged fullerene with silica is dominated by van der Waals forces. For the triply charged fullerenes, electrostatic forces become the principal source of attraction. However, for both positively and negatively charged fullerenes, the preferred location for adhesion is in or adjacent to the hydrophilic (hydrated) regions due to electrostatic attraction to the surface silanol groups.

The charged fullerenes experience increased adhesion with the unmodified polyester surface compared to the neutral C_{60}. Fluorination of the polyester surface leads to improved resistance to C_{60}^{+}, C_{60}^{3+}, and C_{60}^{-} compared to the unmodified polyester. However, C_{60}^{3-} and $C_{60}^{3-(local)}$ exhibit increased adhesion to the fluorinated polyester surface.

The hydroxylated surface shows improved resistance to C_{60}^{+}. However, increased electrostatic attraction and H-bonding leads to increased adhesion between C_{60}^{3+}, C_{60}^{-}, C_{60}^{3-}, and $C_{60}^{3-(local)}$ and the hydroxylated polyester, compared to the unmodified polyester and fluorinated polyester.

Acknowledgment. We gratefully acknowledge the award of an Australian Research Council Linkage Grant in partnership with Bluescope Steel to carry out this work. We acknowledge generous allocations of computing time from both the National Facility of the Australian Partnership for Advanced Computing (APAC) and from the Victorian Partnership for Advanced

Computing (VPAC). We also acknowledge Dr. David Rigby and Mr. Akin Budi for helpful discussions.

References and Notes

(1) See for example: (a) Allman, W. T. *Am. Dyest. Rep.* **1967**, *56*, 761. (b) Reeves, W. A.; Beninate, J. V.; Perkins, R. M.; Drake, G. L. *Am. Dyest. Rep.* **1968**, *57*, 1053−1056. (c) Allman, W. T.; Dunlap, R. K.; Zybko, W. C. *Am. Dyest. Rep.* **1968**, *57*, 1086−1091.

(2) Pósfai, M.; Gelencsér, A.; Simonics, R.; Arató, K.; Li, J.; Hobbs, P. V.; Buseck, P. R. *J. Geophys. Res*. **2004**, *109*, D06213.

(3) Wentzel, M.; Gorzawski, H.; Naumann, K. H.; Saathoff, H.; Weinbruch, S. *Aerosol Sci*. **2003**, *34*, 1347−1370.

(4) Ishiguro, T.; Takatori, Y.; Akihama, K. *Combust. Flame* **1997**, *108*, 231−234.

(5) Ghazaoui, E.; Lindheimer, M.; Lindheimer, A.; Lagerge, S.; Partyka, S. *Colloids Surf. A* **2004**, *233*, 79−86.

(6) Henry, D. J.; Lukey, C. A.; Evans, E.; Yarovsky, I. *Mol. Simul*. **2005**, *31*, 449−455.

(7) Henry, D. J.; Yiapanis, G.; Evans, E.; Yarovsky, I. *J. Phys. Chem. B* **2005**, *109*, 17224−17231.

(8) Petersen, T.; Yarovsky, I.; Snook, I.; McCullock, D. G.; Opletal, G. *Carbon* **2004**, *42*, 2457−2469.

(9) Yiapanis, G.; Henry, D. J.; Evans, E.; Yarovsky, I. In preparation.

(10) See for example: (a) Biryulin, Y. F.; Syckmanov, D. A.; Moliver, S. S.; Orlov, S. E.; Mikov, S. N.; Novoselova, A. V.; Yagovkina, M. A. *Microelectron. Eng*. **2003**, *69*, 505−510. (b) Ren, S.; Yang, S.; Zhao, Y. *Langmuir* **2004**, *20*, 3601−3605.

(11) See for example: (a) Ajie, H.; Alvarez, M. M.; Anz, S. J.; Beck, R. D.; Diederich, F.; Fostiropoulos, K.; Huffman, D. R.; Krätschmer, W.; Rubin, Y.; Schriver, K. E.; Sensharma, D.; Whetten, R. L. *J. Phys. Chem*. **1990**, *94*, 8630−8633. (b) Hamza, A. V.; Balooch, M. *Chem. Phys. Lett*. **1992**, *198*, 603−608. (c) Diack, M.; Compton, R. N.; Guiochon, G. *J. Chromatogr*. **1993**, *639*, 129−140. (d) Wu, Y.; Sun, Y.; Gu, Z.; Wang, Q.; Zhou, X.; Xiong, Y.; Jin, Z. *J. Chromatogr*. **1993**, *648*, 491−496. (e) Gasper, M. P.; Armstrong, D. W. *J. Liq. Chromatogr*. **1995**, *18*, 1047−1076. (f) Gritti, F.; Guiochon, G. *J. Chromatogr. A* **2004**, *1053*, 59−69. (g) Saito, Y.; Ohta, H.; Jinno, K. *Anal. Chem*. **2004**, 267A-272A.

(12) Piwonski, I.; Zajac, J.; Jones, D. J.; Rozière, J.; Partyka, S.; Plaza, S. *Langmuir* **2000**, *16*, 9488−9492.

(13) Kartsova, L. A.; Makarov, A. A. *J. Anal. Chem*. **2004**, *59*, 724−729.

(14) Ban, H.; Schaefer, J. L.; Saito, K.; Stencel, J. M. *Fuel* **1994**, *73*, 1108−1113.

(15) See for example: (a) Gady, B.; Reifenberger, R.; Rimai, D. S.; DeMojo, L. P. *Langmuir* **1997**, *13*, 2533−2537. (b) Rimai, D. S.; Quesnel, D. J.; DeMojo, L. P.; Regan, M. T. J. *Imaging Sci. Technol*. **2001**, *45*, 179−186. (c) Götzinger, M.; Peukert, W. *Powder Technol*. **2003**, *130*, 102−109. (d) Feng, J. Q.; Hays, D. A. *Powder Technol*. **2003**, *135*−*136*, 65−75. (e) Zhou, H.; Götzinger, M.; Peukert, W. *Powder Technol*. **2003**, *135*−*136*, 82−91. (f) Rimai, D. S.; Alexandrovich, P.; Quesnel, D. J. *J. Adhes*. **2003**, *79*, 1041−1066.

(16) Yarovsky, I.; Evans, E. *Polymer* **2002**, *43*, 963−969.

(17) (a) Garofalini, S. H. *J. Chem. Phys*. **1983**, *78*, 2069. (b) Garofalini, S. H. In *Strucutre and Bonding in Noncrystaline Solid*; Walrafen, G. E., Revesz, A. G., Eds.; Plenum Press: New York, 1985. (c) Feuston, B. P.; Garofalini, S. H. *J. Appl. Phys*. **1990**, *68*, 4830. (d) Athanasopoulos, D. C.; Garofalini, S. H. *J. Chem. Phys*. **1992**, *97*, 3775.

(18) (a) Yarovsky, I.; Aguilar, M. I.; Hearn, M. T. W. *Anal. Chem*. **1995**, *67*, 2145. (b) Yarovsky, I.; Aguilar, M. I.; Hearn, M. T. W. *J. Phys. Chem. B* **1997**, *50*, 10962.

(19) Zhuravlev, L. T. *Langmuir* **1987**, *3*, 316−318.

(20) Sun, H. *J. Phys. Chem. B* **1998**, *102*, 7338−7364.

(21) Andersen, H. C. *J. Phys. Chem*. **1980**, *72*, 2384

(22) Iler, R. K. *The Chemistry of Silica, Solubility, Polymerization, Colloid, and Surface Properties and Biochemistry*; Wiley-Interscience: New York, 1979.

(23) (a) Gauntt, D. L.; Clark, K. G.; Hirst, D. J.; Hegedu, C. R. *J. Coat. Technol.* **2001**, *63*, 25−32. (b) Nalaskowski, J.; Drelich, J.; Hupka, J.; Miller, J. D. *Langmuir* **2003**, *19*, 5311−5317.